Robust Wind and Precipitation Responses to the Mount Pinatubo Eruption, as Simulated in the CMIP5 Models

Citation: Barnes, Elizabeth A., Susan Solomon, and Lorenzo M. Polvani. "Robust Wind and Precipitation Responses to the Mount Pinatubo Eruption, as Simulated in the CMIP5 Models." Journal of Climate 29.13 (2016): 4763–4778. © 2016 American Meteorological Society

As Published: http://dx.doi.org/10.1175/jcli-d-15-0658.1

Publisher: American Meteorological Society

Persistent URL: http://hdl.handle.net/1721.1/107425

Version: Final published version: final published article, as it appeared in a journal, conference proceedings, or other formally published context

Robust Wind and Precipitation Responses to the Mount Pinatubo Eruption, as Simulated in the CMIP5 Models

ELIZABETH A. BARNES

Department of Atmospheric Science, Colorado State University, Fort Collins, Colorado

SUSAN SOLOMON

Department of Earth, Atmospheric and Planetary Sciences, Massachusetts Institute of Technology, Cambridge, Massachusetts

LORENZO M. POLVANI

Department of Applied Physics and Applied Mathematics, and Lamont-Doherty Earth Observatory, Columbia University, New York, New York

(Manuscript received 15 September 2015, in final form 28 March 2016)

ABSTRACT

The volcanic eruption of Mount Pinatubo in June 1991 is the largest terrestrial eruption since the beginning of the satellite era. Here, the monthly evolution of atmospheric temperature, zonal winds, and precipitation following the eruption in 14 CMIP5 models is analyzed and strong and robust stratospheric and tropospheric circulation responses are demonstrated in both hemispheres, with tropospheric anomalies maximizing in November 1991. The simulated Southern Hemisphere circulation response projects strongly onto the positive phase of the southern annular mode (SAM), while the Northern Hemisphere exhibits robust North Atlantic and North Pacific responses that differ significantly from that of the typical northern annular mode (NAM) pattern. In contrast, observations show a negative SAM following the eruption, and internal variability must be considered along with forced responses. Indeed, evidence is presented that the observed El Niño climate state during and after this eruption may oppose the eruption-forced positive SAM response, based on the El Niño–Southern Oscillation (ENSO) state and SAM response across the models. The results demonstrate that Pinatubo-like eruptions should be expected to force circulation anomalies across the globe and highlight that great care must be taken in diagnosing the forced response as it may not fall into typical seasonal averages or be guaranteed to project onto typical climate modes.

1. Introduction

Scientific and popular speculation regarding how volcanoes affect surface climate dates back not only to recent centuries but for thousands of years [see references in the review by Robock (2000)]. Explosive volcanic eruptions can increase the stratospheric sulfur dioxide content, which subsequently oxidizes and forms sulfuric acid particles [Deshler (2008) and references therein]. The volcanic particles absorb near-infrared and infrared radiation (Robock 2000) and thereby heat the stratosphere; they also form a volcanic veil that reflects incoming solar shortwave radiation, resulting in the global average cooling that is one of their signature influences on Earth's climate (Robock 2000; Timmreck 2012).

Tropical eruptions lead to the most long-lasting climatic effects, since any particles formed in the tropics that are too small to fall out will be swept upward and slowly transported throughout the globe in the stratospheric meridional overturning circulation. Volcanic aerosols contribute to midlatitude and polar ozone losses through heterogeneous chemistry involving chlorine and bromine (Solomon 1999) so that contemporary tropical volcanoes can affect temperature gradients (and hence circulation) in the stratosphere not only through

Corresponding author address: Elizabeth A. Barnes, Department of Atmospheric Science, Colorado State University, 1371 Campus Delivery, Fort Collins, CO 80523.
E-mail: eabarnes@atmos.colostate.edu

DOI: 10.1175/JCLI-D-15-0658.1

direct tropical warming associated with the particles but also through indirect higher-latitude cooling due to ozone depletion (Stenchikov et al. 2002). Enhanced stratospheric loadings decay exponentially over time scales on the order of 1–2 years [see review by Deshler (2008) and references within]. Numerical simulations using individual climate models were shown to broadly reproduce the observed volcanic stratospheric warming and wind anomaly patterns more than 20 years ago (Graf et al. 1993; Perlwitz and Graf 1995; Kodera et al. 1996), after the eruption of Mount Pinatubo in 1991, one of the largest tropical eruptions of the twentieth century.

Detailed analysis of historical eruptions has demonstrated that despite globally averaged cooling, the winters following major tropical volcanic eruptions tend to be anomalously warm in high northern latitudes (Robock and Mao 1995; Graf et al. 1993; Christiansen 2008) because of changes in the patterns of tropospheric circulation, particularly the North Atlantic Oscillation (NAO) and, in some studies, the northern annular mode (NAM). While some individual climate model studies reported success in simulating Northern Hemisphere (NH) tropospheric responses (e.g., Graf et al. 1993; Stenchikov et al. 2002; Rozanov et al. 2002; Thomas et al. 2009), the availability of a broader range of multimodel climate ensemble results has not yielded a fully consistent picture. Driscoll et al. (2012) argue that tropospheric NH responses to multiple composited eruptions are unclear or too weak compared to observations in the models used in phase 5 of the Coupled Model Intercomparison Project (CMIP5; Taylor et al. 2012). The basic mechanism linking volcanic eruptions to tropospheric circulation changes is thought to arise from a strengthening of the winter polar vortex that affects the propagation of planetary waves (Perlwitz and Graf 1995). Ottera (2008) and Stenchikov et al. (2006) argue that overly strong polar vortices in many models could impede the signal of volcanic forcing. The CMIP5 ensemble forms the basis for a study by Ding et al. (2015), who argue for a key role of oceanic responses in NAO linkages to volcanic eruptions, particularly through sea ice changes as well as changes in the ocean circulation, and note important differences in ocean responses among models.

Only a few studies have explored linkages between volcanic eruptions and the southern annular mode (SAM). Roscoe and Haigh (2007) examined the influences of ozone depletion, the solar cycle, the quasi-biennial oscillation (QBO), and volcanoes on the SAM using observations and regression techniques. They concluded that the stratospheric circulation and SAM strengthen, as in the NH, but suggested a negative SAM in the troposphere. Robock et al. (2007) found no response of the SAM in the stratosphere or troposphere to the Pinatubo eruption in the NASA GISS model and suggested that the SH response could be weaker than the NH response because of a "more steady jet and vortex." Karpechko et al. (2010) analyzed the composite responses to the El Chichón and Pinatubo eruptions in the suite of models in phase 3 of the Coupled Model Intercomparison Project (CMIP3) and found a significant response projecting on the positive phase of the SAM in both the stratosphere and troposphere during austral spring and autumn following the eruptions.

In this paper, we examine circulation and precipitation responses in the CMIP5 model ensemble following the eruption of Mount Pinatubo, using methodologies aimed at elucidating stratosphere–troposphere coupling. The evolution of ozone depletion has affected the structure of the stratosphere since the mid-1980s, particularly in the Antarctic ozone hole region where it has altered the strength of the stratospheric vortex and SAM [Thompson et al. (2011) and references therein]. Muthers et al. (2014) suggest that the circulation response to volcanic eruptions is nonlinearly sensitive to the model ozone climatology through modulation of the strength of the stratosphere–troposphere coupling. These findings suggest that compositing volcanoes from the pre-ozone-depletion era and more recent volcanoes may not be appropriate and motivate our examination of the Pinatubo period alone since it is the largest tropical eruption that has occurred since ozone depletion developed. Further, we show that the Pinatubo signal evolves rapidly in space and time in both the stratosphere and troposphere. Rather than examining winter season averages as in a number of previous studies, we consider the detailed monthly time evolution and show that this allows the identification of signals in SAM, NAM, NAO, and tropical precipitation that are robust. Section 2 describes the data and methods to be used in this paper. Sections 3 and 4 present circulation, precipitation, and annular mode responses obtained in the model ensemble, while sections 5 and 6 present a discussion and the conclusions of our work.

2. Data and methods

a. CMIP5 model output

We analyze model integrations performed for CMIP (Taylor et al. 2012). Specifically, we focus on 25 years of the historical integrations (1980–2004) of the subset of the CMIP5 models that exhibit reasonable lower-stratospheric temperature responses to volcanic forcings as identified by Santer et al. (2013b, their Fig. S1). By reasonable, we mean that globally averaged lower-stratospheric temperature anomalies exceed 0.5°C following the eruption [the observed anomaly was approximately 1.5°C; see Santer et al. (2013a), their

TABLE 1. CMIP5 models used in this analysis and their abbreviations.

Model	Abbreviation
BCC_CSM1.1	bcc1
CanESM2	cane
CCSM4	ccsm
CNRM-CM5	cnrm
CSIRO Mk3.6.0	csir
GFDL CM3	gcm3
GISS-E2-H	ge2h
GISS-E2-R, p1	ge2r_p1
GISS-E2-R, p3	ge2r_p3
HadGEM2-ES	hade
MIROC-ESM	mire
MIROC-ESM-CHEM	mirc
MRI-CGCM3	mric
NorESM1-M	norm

Fig. S3]. The 13 models analyzed in this study are listed in Table 1. Only the first ensemble member is used for each model in order to give equal weight across the 13 models. While previous studies have averaged all available runs for each model, we find that one run each is enough to extract a clear circulation response to the Pinatubo eruption and avoids biases due to uneven weighting across different models that may have different numbers of runs. The exception is GISS-ER-R, where we additionally use the third run (p3) since interactive ozone chemistry is turned on in this run but was off for the first run (p1). Thus, we analyze 14 separate historical simulations. We restrict the focus of this analysis to three key variables: monthly mean zonal wind, atmospheric temperature, and precipitation. Because of the differences in model grid spacing, all fields for all models are linearly interpolated to a 2° by 2° latitude–longitude grid before any analysis is performed.

As detailed in Maher et al. (2015, their Table S1), a single volcanic forcing was not specified for CMIP5, resulting in five different input aerosol forcing datasets being used across the CMIP5 models. Since we are interested in the multimodel mean circulation response rather than the behavior of each model individually, we make no attempt here to compare the responses as a function of volcanic forcing dataset. Furthermore, Maher et al. (2015) compared the tropical circulation responses to volcanic eruptions between models that used different aerosol forcing datasets; while some differences were noted, their overall conclusion was that the tropical circulation response was robust to the model treatment of volcanic aerosol.

b. *Defining seasonal anomalies*

The 25-yr climatological base period used throughout this study spans 1980–2004, and it is this period that is used to define all anomalies. Because of the effects of stratospheric ozone loss on the tropospheric circulation during that period (e.g., Barnes et al. 2014), one might be concerned that the results will be sensitive to this base period; however, we have verified that the conclusions are not sensitive to this choice. Monthly anomalies are defined as deviations from the climatological seasonal cycle, where the seasonal cycle is defined as the average over the base period for each of the 12 months. Finally, we remove any linear trend. We note, however, that the results are unchanged if the linear trend is retained.

c. *Annular mode definitions*

The SAM and NAM are defined for each model, at each pressure level, as the leading EOF of the monthly mean zonally averaged anomalous zonal winds between 20° and 80° latitude of the respective hemispheres. The leading principal components (the annular mode time series) are standardized by subtracting the 1980–2004 mean value and dividing by the standard deviation. As is convention, a positive tropospheric annular mode index is defined such that the jet stream is strengthened and shifted poleward relative to climatology. In the stratosphere, a positive value denotes strengthened zonal winds (vortex) relative to climatology (e.g., Baldwin and Dunkerton 1999). Observed SAM, NAM, and NAO indices were computed following the same procedure as for the CMIP5 models but using the zonal wind from the Modern-Era Retrospective Analysis for Research and Applications (MERRA) data (Rienecker et al. 2011).

d. *Statistical significance*

Here, we take two approaches to assessing the significance of the multimodel mean responses. The first is a bootstrap approach (Efron 1979). Specifically, we create 5000 synthetic anomalies for each model for each month by randomly sampling from the 25 values of that respective month over the 1980–2004 period. The multimodel average is calculated for each of the 5000 synthetic datasets for each month, and the two-sided 95% confidence interval on the multimodel mean response is determined as the 2.5–97.5th-percentile range of the 5000 synthetic means. We note that the autocorrelation of the monthly SAM and NAM time series is small (typical e-folding times of less than 2 months), and thus, we have assumed no memory in our bootstrap analysis.

The second approach quantifies the level of model agreement in the sign of the response. Although the multimodel mean response may be small, if all of the models agree on the sign of the response, one might be more inclined to believe it is physically robust. On the other hand, even if the multimodel mean response is large, the model agreement may still be small, possibly highlighting that the multimodel mean response is

dominated by only a few models. In the figures that follow, we define a robust response as one where at least 80% of the simulations (at least 11 of 14) agree on the sign of the response. If the data were purely random, we would expect at least 11 of the 14 models to agree on the sign of the response 5.7% of the time, similar to the typical 95% confidence limit.

By diagnosing significance using a combination of these two approaches, bootstrap resampling and model agreement, we assess significance from both the multimodel and individual model perspectives.

3. Circulation response to Pinatubo

a. *Temporal evolution of zonal-mean wind and temperature response*

In the CMIP5 models, significant zonal wind and temperature anomalies are found in both hemispheres following the Pinatubo eruption. This can be seen in Fig. 1, where time progresses from top to bottom starting with the left-hand panel. Figure 1 (top left) shows the model mean zonal wind (shading) and temperature (contours) anomalies for July 1991 (the month following the 15 June eruption) and time progresses down the column. The stratospheric zonal wind response is in thermal wind balance with the temperature anomalies, which exhibit the well-known warming in the lower equatorial stratosphere (e.g., Robock 2000). In the Southern Hemisphere, the initial stratospheric zonal wind anomalies in July 1991 lie near 40°S and shift poleward over the following months as the tropical warming intensifies. Polar cooling accompanies the tropical warming (apparently because of changes in the meridional circulation). By November 1991, the polar stratospheric vortex has strengthened and these anomalies extend all the way to the pole. This migration of the stratospheric wind anomalies can be seen to a lesser extent in the Northern Hemisphere as well, where the initial positive stratospheric wind anomaly in August 1991 lies between 20° and 40°N, and then shifts poleward over the subsequent months until the strengthened stratospheric vortex extends to the pole in November 1991.

In the month following the eruption (July 1991), a robust tropospheric zonal wind response is also seen in both hemispheres, with positive zonal wind anomalies suggestive of poleward shifts of the tropospheric, midlatitude jet streams. As time progresses through August and September, the tropospheric midlatitude zonal wind anomalies weaken substantially and the reason for this will be discussed further in section 5. By October and November, robust dipolar anomalies once again emerge in both hemispheres, extending from the top of the stratosphere all the way to the surface. By January and February 1992, the zonal wind anomalies in both hemispheres weaken substantially and lose their significance, although an increase in the tropical tropospheric zonal winds begins to emerge during this time.

These results demonstrate that significant zonal wind anomalies are simulated by the CMIP5 models in response to the Pinatubo eruption in both hemispheres and that the responses are relatively symmetric, showing positive zonal winds on the poleward flanks of the climatological jet streams and negative zonal winds on the equatorward flanks. In a later section, we will demonstrate the extent to which these anomalies project onto the hemispheric annular modes.

b. *Precipitation response*

The zonal winds and temperatures are not the only features that exhibit a robust response to Pinatubo in the CMIP5 models. Changes in precipitation are also seen in the tropics following the eruption, as seen in Fig. 2a. The black contours show the seasonal march of precipitation, and the colors denote anomalous precipitation about this seasonal cycle. Significant precipitation anomalies are seen in the tropics (stippling), representing an enhancement of precipitation north of the equator and a decrease south of the equator. Robust precipitation anomalies are also found in the midlatitudes. In the Southern Hemisphere midlatitudes (around 40°–60°S) following the eruption, a poleward shift of precipitation is found in the majority of models (out of phase anomalies straddling the climatological mean region of enhanced precipitation), which is consistent with the poleward shift of the storm tracks as discussed previously. A similar poleward shift in precipitation is seen in the Northern Hemisphere in early winter of 1991, centered near 50°N.

The main precipitation features seen in the multimodel mean response are also seen in the individual models, as quantified by the model agreement in Fig. 2b. Dark cool colors reflect that the majority of models agree on a wetting there, while dark warm colors reflect a drying. Thus, we can interpret the precipitation anomalies in Fig. 2a as also representative of the individual model responses.

c. *Zonal asymmetries in the response*

Thus far, our diagnostics have focused on zonal-mean anomalies alone. However, Figs. 3 and 4 demonstrate a large degree of zonal asymmetry in the zonal wind responses in the stratosphere (50 hPa; Fig. 3) and troposphere (500 hPa; Fig. 4). An initial stratospheric response of the zonal winds is seen only in the Southern Hemisphere (July 1991), and the anomalies appear in a wave-2 pattern. By October, the Southern Hemisphere anomalies

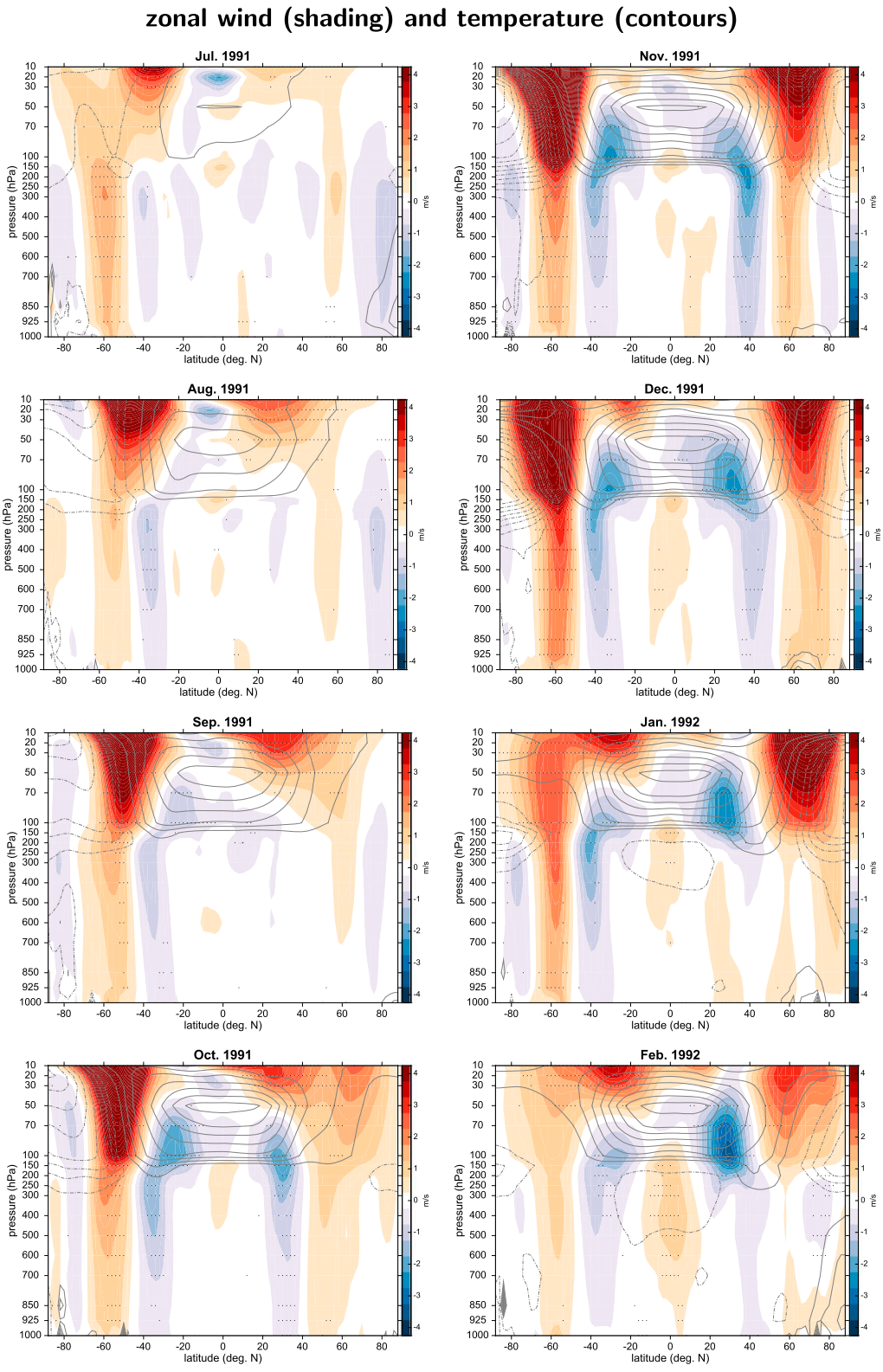

FIG. 1. Pressure–latitude cross sections of the multimodel mean zonal wind (shading) and temperature anomalies (contours) for the months following Pinatubo. Temperatures are contoured every 0.5 K. Stippling denotes regions where at least 80% of the simulations (at least 11 of 14) agree with the sign of the multimodel mean wind response.

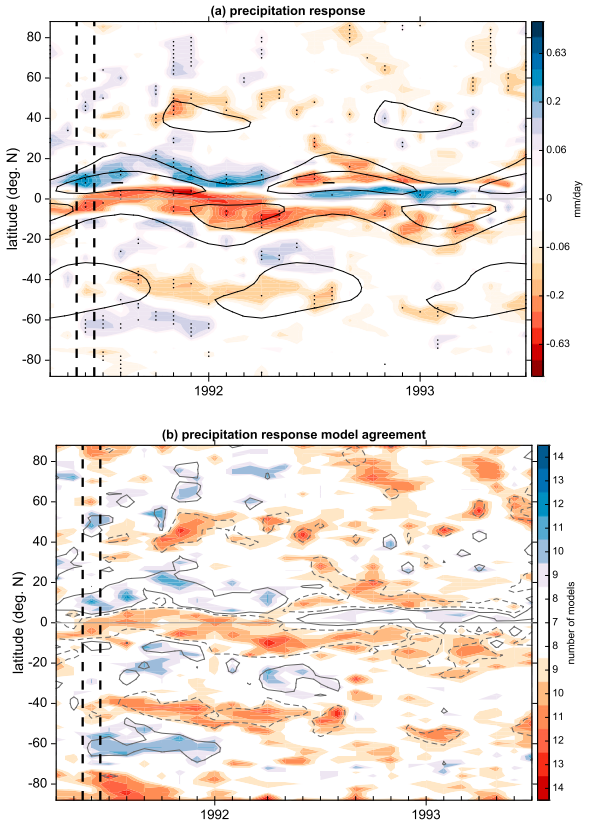

FIG. 2. (a) Multimodel mean precipitation anomalies as a function of latitude following the Pinatubo eruption (denoted by the vertical dashed lines). Stippling denotes anomalies statistically different from zero at the 95% confidence level. Contours denote the multimodel mean seasonal cycle of precipitation, contoured every 3 mm day^{-1}. (b) Model agreement in the precipitation anomalies, where warm colors denote regions where more than half of the models exhibit drying and cool colors denote regions where more than half of the models exhibit wetting. Contours denote the ± 0.08 mm day^{-1} multimodel mean precipitation anomaly from (a). Vertical dashed lines denote June 1991.

become largely zonal and extend around the hemisphere. Robust Northern Hemisphere stratospheric wind anomalies appear two months after the eruption and move poleward throughout the following months. However, these anomalies are distinctly nonzonal, exhibiting a wave-2 pattern through February 1992.

Robust tropospheric wind anomalies appear in the Southern Hemisphere (Fig. 4), with the largest at the tip of South America. As time passes, the anomalies become more widely spread across longitudes but almost never display a purely zonal response except, perhaps, in December 1991. In the Northern Hemisphere, deviations from zonal symmetry are even more pronounced, as one might expect because of the zonal asymmetries in the jet streams driven by the distribution of land. By winter (November–January), two distinct regions of action emerge—one over the North Atlantic, indicative of a positive NAO pattern, and another, more poleward, over the North Pacific.

4. Annular mode response to Pinatubo

a. SAM and NAM responses

The response of the circulation to volcanic eruptions has been typically quantified by the SAM or NAM/NAO response in the literature. We have also performed such an analysis, and the results for the Southern Hemisphere SAM are plotted in Fig. 5a, where time is plotted along the *x* axis from May 1991 to June 1993 and vertical dashed lines denote June 1991, the month of the eruption. Warm colors correspond to a positive SAM index, or a poleward-shifted jet stream. Figure 5a displays a significant positive SAM anomaly that propagates from the stratosphere into the troposphere in the months following the eruption. The stratospheric signal is seen immediately following the eruption and is sustained through December 1991, with weaker lingering effects throughout the following year. In the troposphere, a weak but significant positive SAM anomaly is also seen immediately following the eruption; however, the strongest tropospheric SAM anomaly occurs in November and December, 5–6 months following the eruption. The models largely agree on the positive SAM response following Pinatubo, as one can see in Fig. 5b. Thus, the multimodel mean at least qualitatively captures a robust positive SAM response in the months following the eruption.

The simulated NAM response is markedly different to that of the SAM. While the Northern Hemisphere stratosphere also exhibits a positive NAM response (akin to that of the Southern Hemisphere), the signal does not appear until approximately 5 months after the eruption (Fig. 5c). Furthermore, the multimodel mean NAM response in the troposphere is weak, although there is some evidence of model agreement on the sign of the NAM response in the lower troposphere in October–December (Fig. 5d). It may seem that these results contradict the robust circulation responses that were shown in the Northern Hemisphere in Figs. 1 and 4. However, we will next demonstrate that while there are certainly robust responses throughout the Northern Hemisphere, they are simply not well captured by the NAM index.

b. Alternative metric for diagnosing the circulation response

In the preceding section, the circulation response was quantified using an annular mode index. In other words, we quantified how much the zonal wind anomalies look

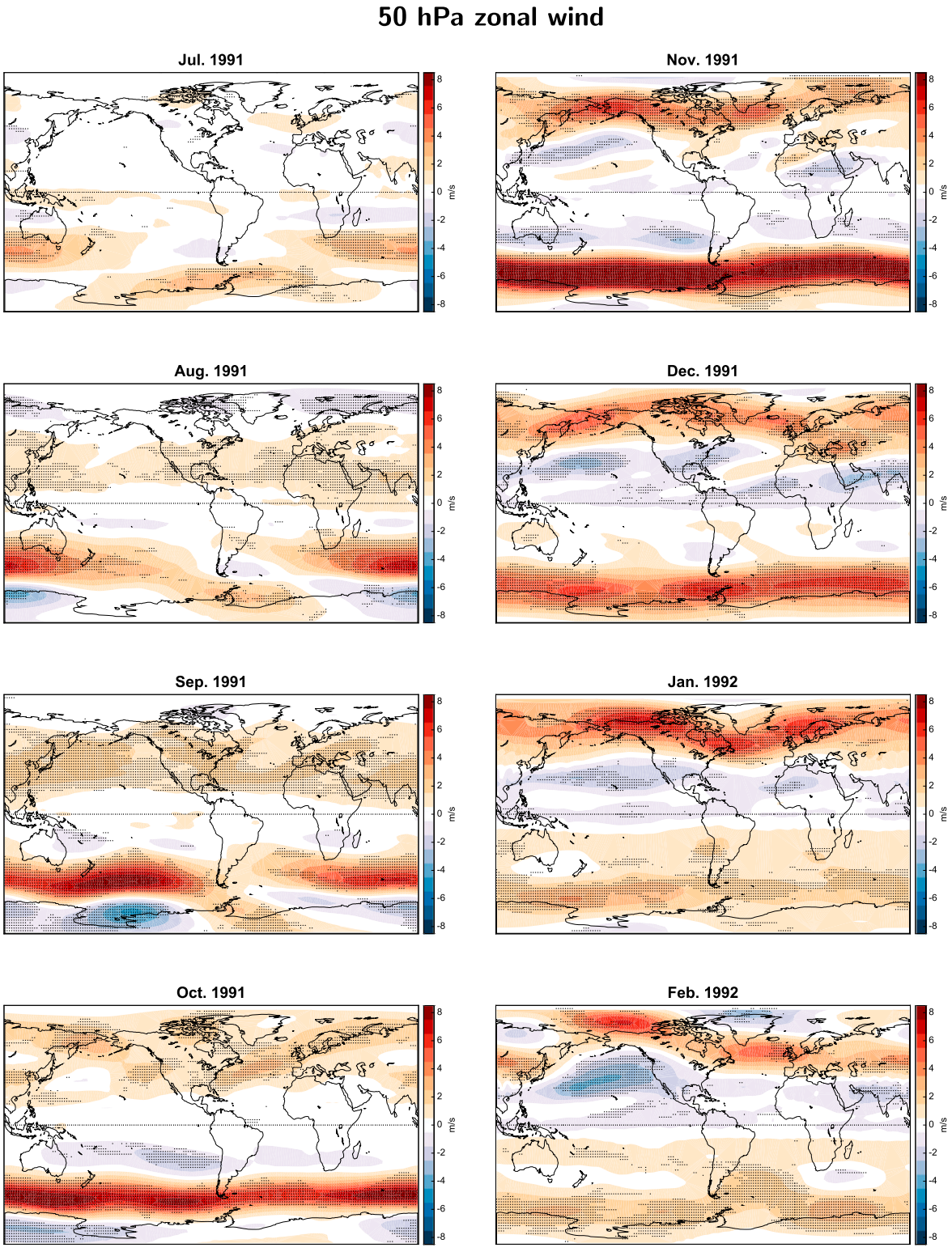

FIG. 3. Latitude–longitude cross sections of the multimodel mean 50-hPa zonal wind anomalies for the months following Pinatubo. Stippling denotes regions where at least 80% of the simulations (at least 11 of 14) agree on the sign of the response.

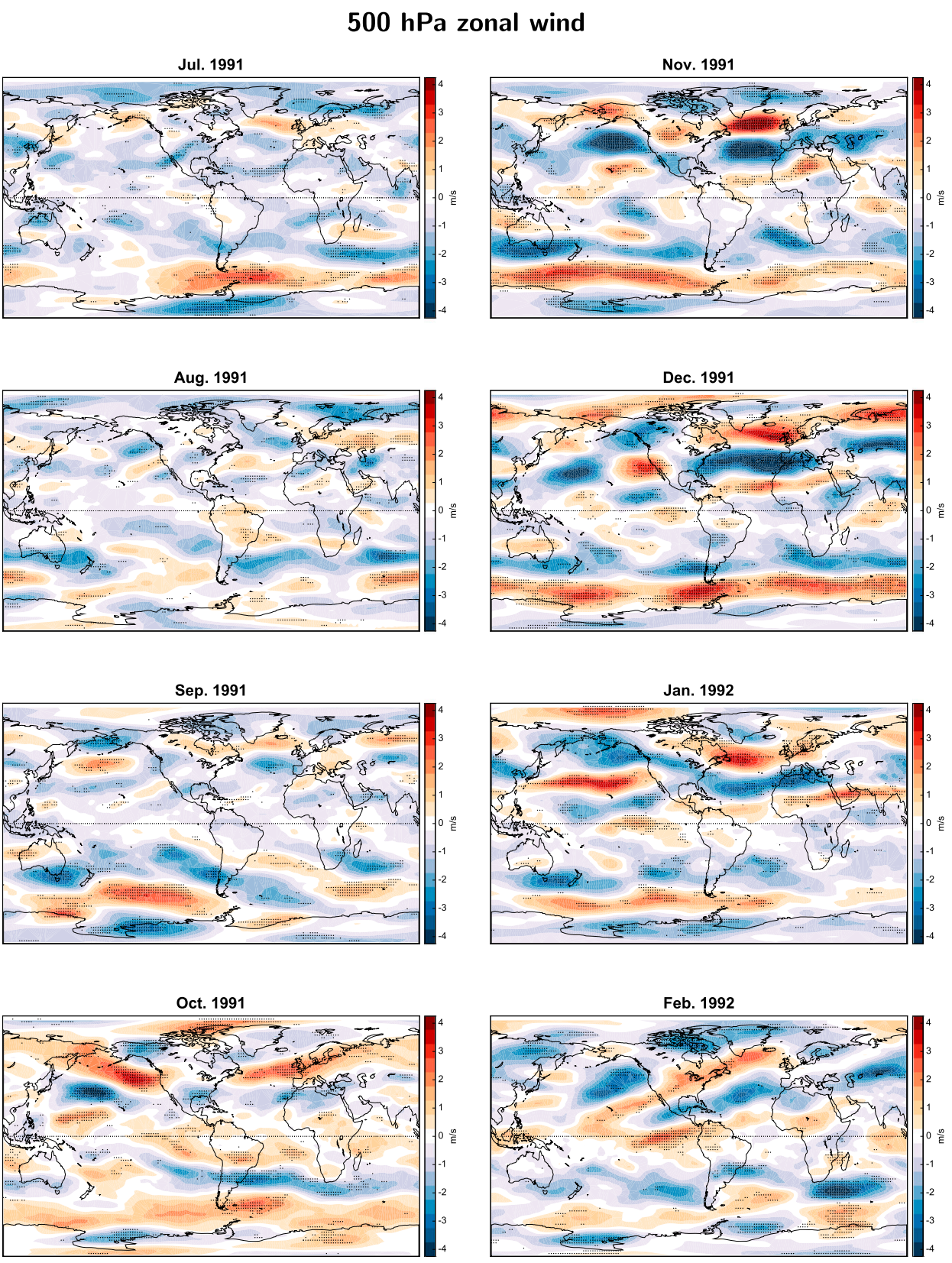

FIG. 4. Latitude–longitude cross sections of the multimodel mean 500-hPa zonal wind anomalies for the months following Pinatubo. Stippling denotes regions where at least 80% of the simulations (at least 11 of 14) agree on the sign of the response.

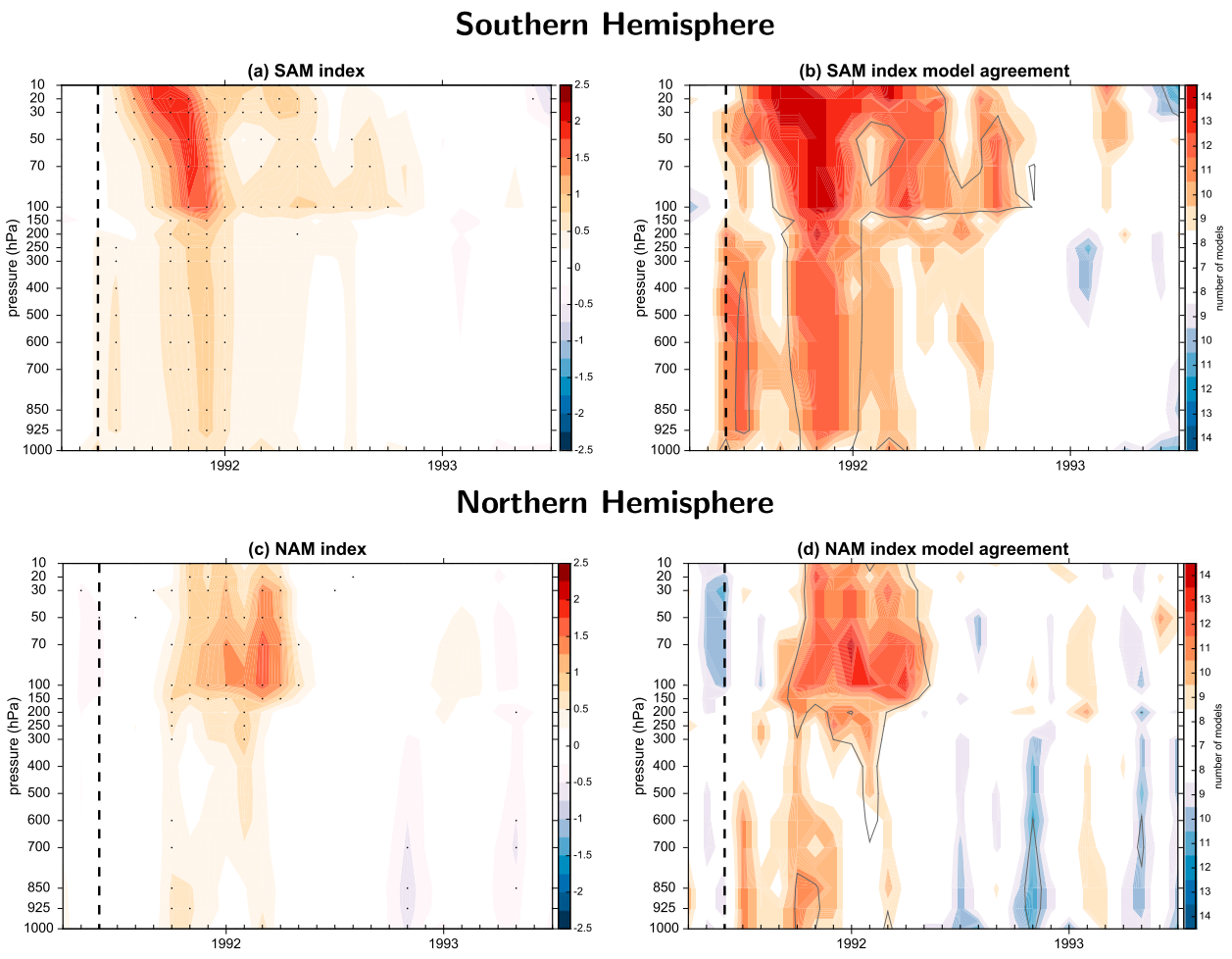

FIG. 5. (a),(c) The multimodel mean zonal wind SAM and NAM indices following the Pinatubo eruption (denoted as the vertical dashed lines), with stippling denoting values significant at the 95% confidence level using a bootstrap approach. (b),(d) Model agreement in the SAM and NAM response following the Pinatubo eruption. Warm colors denote regions where more than half of the models exhibit positive SAM responses, and cool colors denote regions where more than half of the models exhibit negative SAM responses. The gray contour denotes the ±0.5 multimodel mean index response from (a). Vertical dashed lines denote June 1991.

like the canonical SAM/NAM pattern. Figure 6 shows examples of the zonal-mean zonal wind anomalies for the Southern and Northern Hemispheres in months following the eruption. The solid lines show the multimodel mean zonal wind anomaly, and the dashed lines show the multimodel mean annular mode anomaly pattern. For the Southern Hemisphere in November (Fig. 6a), the 500-hPa zonal wind response aligns well with the SAM pattern, which is also reflected in the significant 500-hPa SAM anomaly during this month (Figs. 5a,b). On the other hand, Fig. 6b demonstrates that while the 150-hPa anomaly also exhibits a dipolar structure in September, it is shifted poleward with respect to the SAM pattern at this pressure level. Because of this offset, the SAM index in September 1991 is small and not significant at 150 hPa (see Figs. 5a,b), although a significant dipolar anomaly is actually present. A lack of alignment between the dipolar response and the annular mode is also found in the Northern Hemisphere in November at 500 hPa (Fig. 6c), and this is further reflected in Figs. 5c and 5d.

Because of the inability of the SAM/NAM pattern to capture aspects of the simulated circulation anomalies following the Pinatubo eruption, we have developed a simple diagnostic for quantifying the dipolar response of the circulation without the use of a SAM/NAM pattern. Our aim here is not to develop an exhaustive diagnostic for quantifying all circulation responses but rather to find the simplest diagnostic that can capture both the Southern Hemisphere and Northern Hemisphere zonal wind responses. The diagnostic is calculated as follows: First, for each model, month, and pressure level, we define the ''poleward node'' as the largest zonal wind anomaly (either positive or negative)

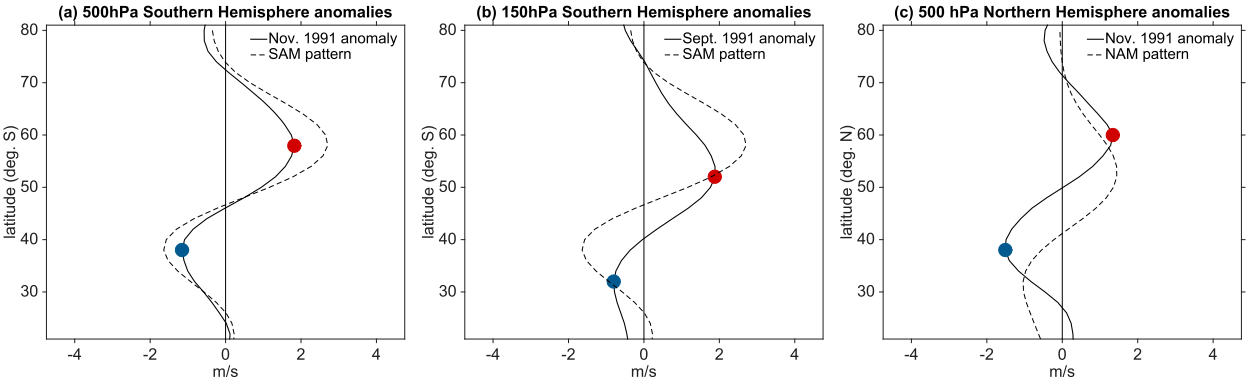

FIG. 6. The multimodel mean anomalous zonal winds following the Pinatubo eruption for Southern Hemisphere (a) 500-hPa anomalies in November 1991 and (b) 150-hPa anomalies in September 1991 and (c) Northern Hemisphere 500-hPa anomalies in November 1991. Poleward and equatorward nodes are denoted by red and blue dots, respectively.

between 45° and 75° latitude and define the "equatorward node" as the largest zonal wind anomaly (either positive or negative) between 15° and 45° latitude. Extrema that occur on the edges of the domain are not considered. Examples of poleward and equatorward nodes are plotted as blue and red dots, respectively, in Fig. 6. Second, we average the magnitudes of these nodes over all models, and this results in the multimodel mean node magnitude as a function of month and pressure. Note that one can instead first calculate the multimodel mean zonal wind anomaly profiles and then determine the poleward and equatorward nodes from this multimodel mean pattern. We have performed such a calculation and the results are similar; however, we have chosen to show the mean of the individual model results in order to be consistent with the SAM/NAM analysis and to ensure that no one model dominates the response.

The results of the anomaly node calculation are shown in Fig. 7, where stippling denotes values statistically different from zero using a one-sided 95% bootstrap test. Multiple key conclusions can be drawn from these panels, and so we take a moment to discuss them in detail, beginning with the results for the Southern Hemisphere. The poleward node magnitude (Fig. 7a) looks very similar to that of the SAM index seen in Fig. 5a, with a positive poleward anomaly appearing in the stratosphere soon after the eruption and then propagating down into the troposphere where it maximizes and reaches the surface in the following winter (approximately 5–7 months following the eruption). This signal differs significantly from that of the negative equatorward anomaly (Fig. 7b), which is significantly weaker than that of the poleward anomaly in the stratosphere and near the surface, with the magnitude maximizing around the tropopause. We note that it is not too surprising that the equatorward anomaly is weak in the stratosphere since stratospheric anomalies associated with the SAM are not dipolar but rather are largely of one sign (not shown). Thus, even for a pure stratospheric annular mode response, there would be no equatorward node to capture.

Recall that the simulated NAM response showed few significant tropospheric anomalies following the Pinatubo eruption (Fig. 5c). The Northern Hemisphere poleward node magnitude (Fig. 7c), however, shows a clear and significant zonal wind response that propagates from the stratosphere down to the surface the following winter, when the Southern Hemisphere tropospheric response also maximizes (Fig. 7a). Furthermore, we see a significant equatorward anomaly (Fig. 7d) that also propagates into the troposphere and maximizes at the same time. One might think that this contradicts the lack of positive NAM response seen in Figs. 5c and 5d; however, this is not the case, since the dipolar anomalies are shifted poleward with respect to the NAM pattern (e.g., Fig. 6b) and thus are not captured by the NAM index.

Since, as already noted, the circulation response to Pinatubo is highly zonally asymmetric (Figs. 3 and 4), it is instructive to perform a similar anomaly node calculation for the zonal wind over the North Pacific (120°–240°E) and North Atlantic (250°–70°E) basins separately; we plot the results in Fig. 8. While this definition of the North Atlantic extends well into western Russia, we have chosen this domain to be consistent with that used by Driscoll et al. (2012) and Christiansen (2008). The North Atlantic exhibits a robust positive poleward and negative equatorward zonal wind anomaly in the winter following the eruption, in agreement with observations and modeling studies that depict a positive NAO response following a volcanic eruption (e.g., Christiansen 2008; Ortega et al. 2015). In addition, we see a similarly robust circulation response in the North Pacific depicting a poleward shift of

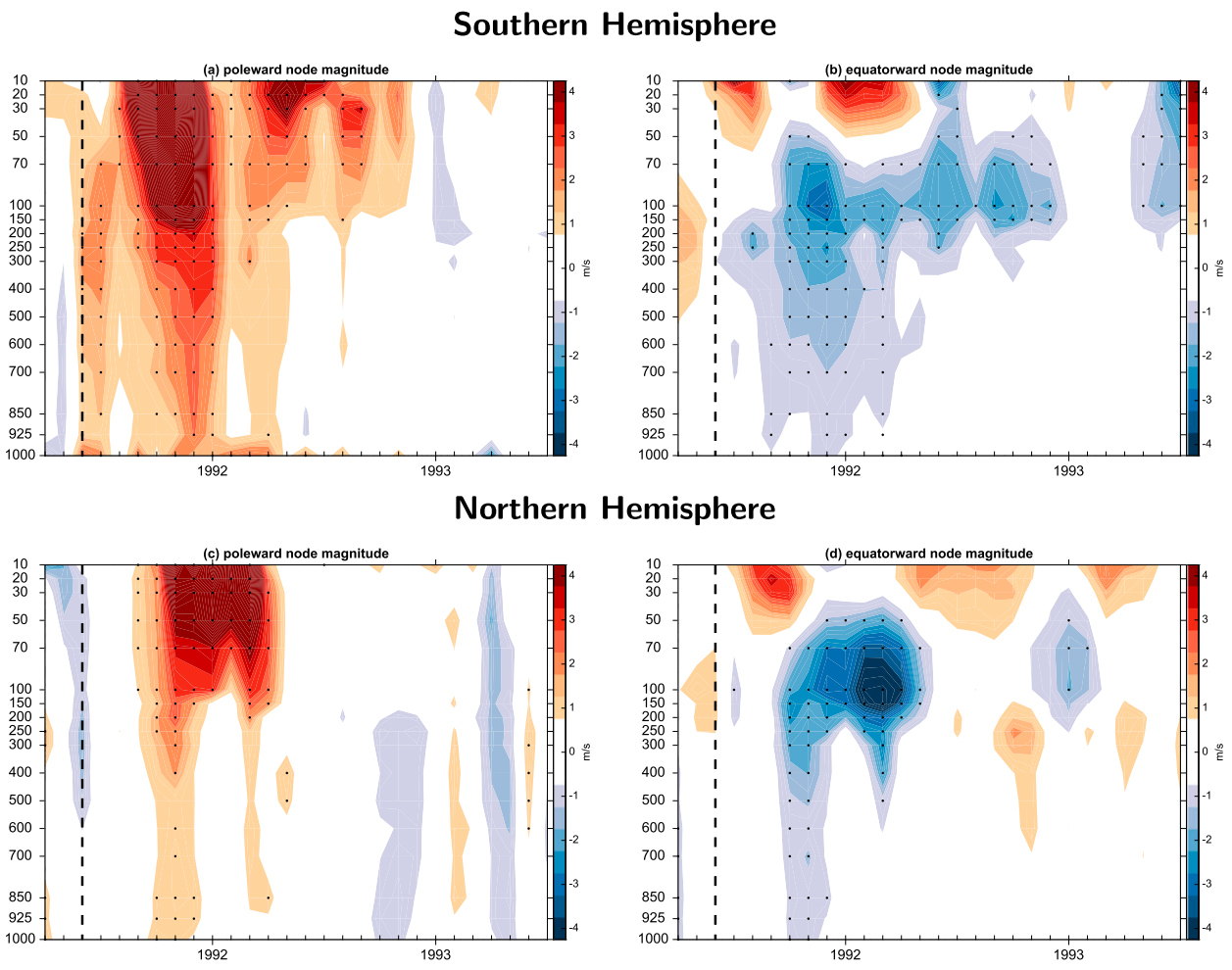

FIG. 7. Multimodel mean magnitude of the zonal wind (a),(c) poleward (45°–75° latitude) and (b),(d) equatorward (15°–45° latitude) nodes following the Pinatubo eruption for the (top) Southern Hemisphere and (bottom) Northern Hemisphere. Stippling denotes values statistically different from zero using a one-sided 95% confidence bootstrap test. Vertical dashed lines denote June 1991.

the tropospheric jet stream in early winter and late winter/early spring following the eruption (Figs. 8c,d). In January, however, this pattern flips sign, although it is no longer significant. The reason for this midwinter reduction and change in sign of the anomalies is likely due to the poleward propagation of the positive/negative anomaly pair over the North Pacific between November and January as seen in Fig. 4. Thus, the poleward anomaly between 45° and 75°N is positive in November but is negative in December.

Both the North Pacific and North Atlantic exhibit strong, robust circulation anomalies in the CMIP5 simulations, although these anomalies do not project onto the NAM index since the North Pacific anomalies are displaced poleward (recall Fig. 4). Thus, the finding by Christiansen (2008) that the NAO response is stronger than that of the NAM is likely a reflection of the inability of the NAM to capture the response at all longitudes rather than an indication of a dominance of the forced anomalies in the North Atlantic.

5. Discussion of climate variability

We now move from a discussion of the CMIP5 models to the reanalysis. Following the eruption of Mount Pinatubo, the observed Southern Hemisphere circulation was in a negative SAM state over the following year, as shown in Fig. 9a for MERRA (red line). This is in direct contrast to the results we have shown for the CMIP5 models—namely, that the response of the circulation in both hemispheres is that of a positive SAM and NAM/NAO. However, although the CMIP5 ensemble shows a robust SAM and NAO response in the months following the Pinatubo eruption (black dots), there is still a large spread in the magnitude of the individual model responses (gray curves). Moreover, it is

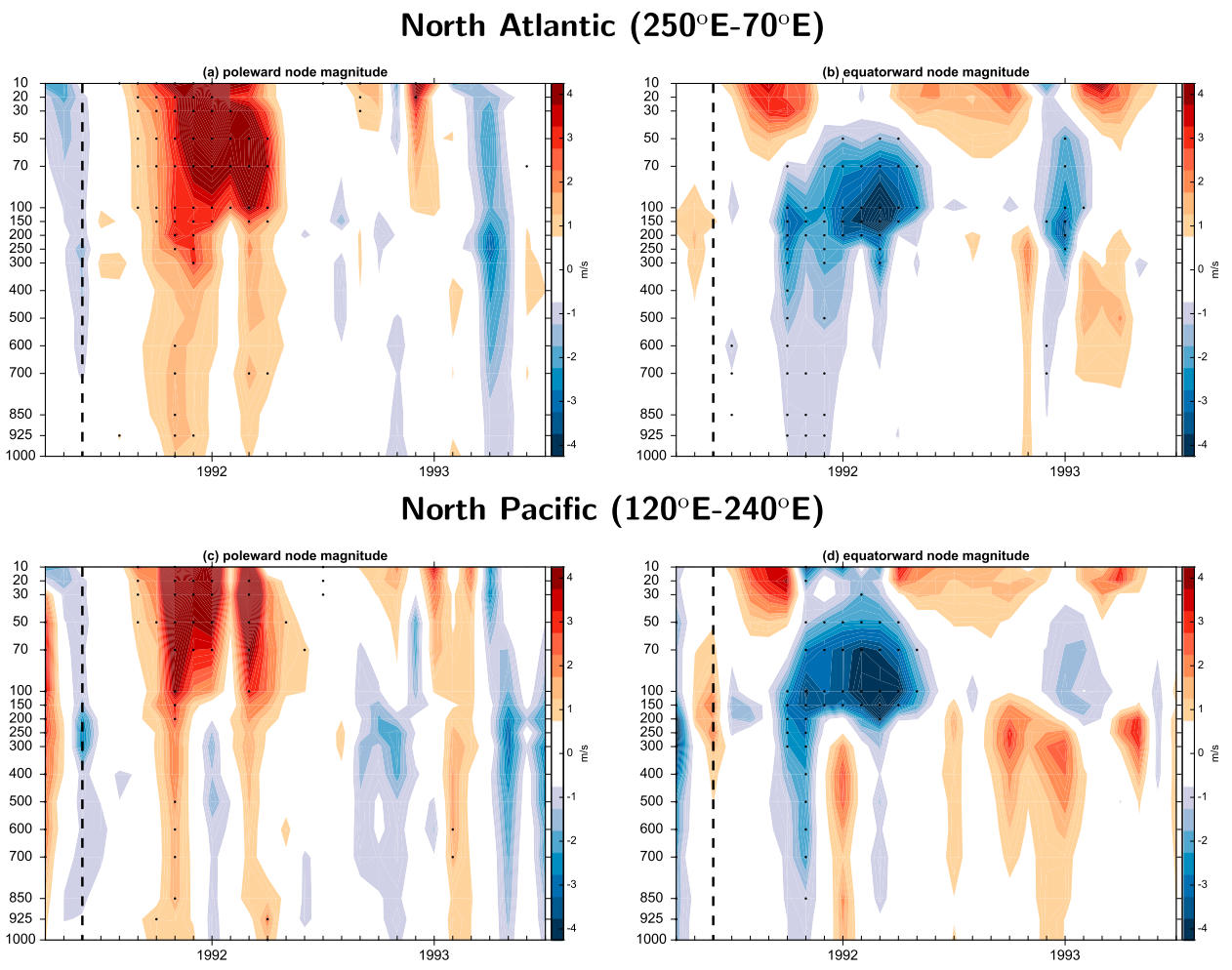

FIG. 8. Multimodel mean magnitude of the zonal wind (a),(c) poleward (45°–75° latitude) and (b),(d) equatorward (15°–45° latitude) nodes following the Pinatubo eruption for the (top) North Atlantic and (bottom) North Pacific. Stippling denotes values statistically different from zero using a one-sided 95% confidence bootstrap test. Vertical dashed lines denote June 1991.

well established that large volcanic eruptions tend to force a positive NAM/NAO response over the following two years, and yet, there is still a large amount of variability in the observed NAM/NAO index following the Pinatubo eruption (Figs. 9b,c). These results suggest that although the forced circulation response to Pinatubo appears to be a positive annular mode pattern [as simulated by the CMIP5 models and consistent with the CMIP3 model results of Karpechko et al. (2010)], this forced response may be difficult to detect in the observations in the presence of climate variability.

Indeed, internal climate variability may explain why unlike the simulated positive SAM response in the CMIP5 models, the observations show a negative SAM following Pinatubo (Fig. 9a). While the observed negative SAM has led some studies to suggest that volcanic eruptions may force the circulation into a negative SAM state (e.g., Roscoe and Haigh 2007), other studies have suggested that the El Niño state during and immediately following the eruption may have hidden the forced positive SAM response (e.g., Karpechko et al. 2010). The circulation response to El Niño is a negative SAM-like pattern (e.g., L'Heureux and Thompson 2006), and thus, this may have partially or entirely canceled the positive SAM response to the Pinatubo eruption. Indeed, a recent study by Lehner et al. (2016) suggests that the El Niño state may have muted the observed global mean temperature response to the Pinatubo eruption.

To explore this hypothesis in the CMIP5 models, we quantify the monthly El Niño–Southern Oscillation (ENSO) state in each model by computing the monthly mean Niño-3.4 index, defined as the average tropical Pacific sea surface temperatures between 5°N and 5°S and 170° and 120°W. A positive Niño-3.4 index implies an El Niño event, while a negative index implies a La Niña event. The observed monthly mean Niño-3.4 index is

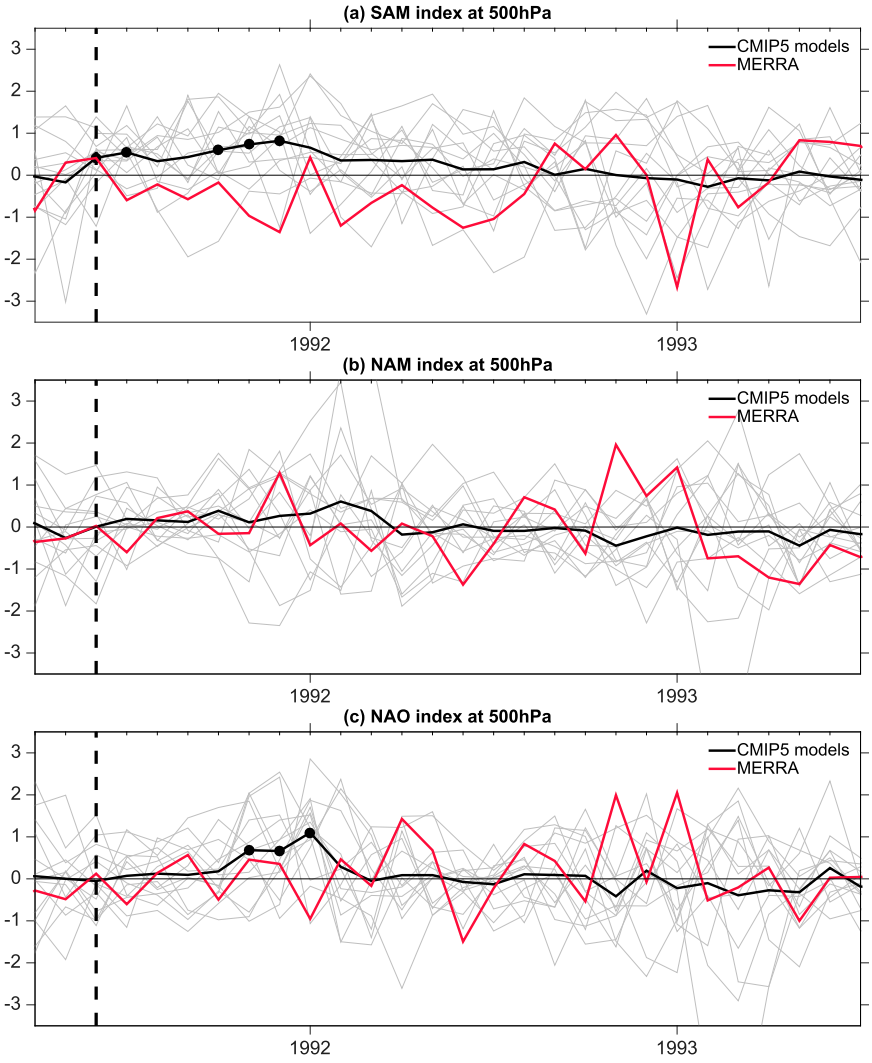

FIG. 9. Time series of the monthly 500-hPa (a) SAM, (b) NAM, and (c) NAO indices from the CMIP5 models (gray lines) and MERRA (red lines). Thick black lines denote the CMIP5 multimodel mean, and black dots denote months where at least 80% of the models (at least 11 of 14) agree on the sign of the change.

obtained from NOAA's Earth System Research Laboratory. Figure 10 shows the average Niño-3.4 index in the 3 months following the eruption (June–August 1991) in colors for each model and MERRA. We average over June–August to ensure an early enough period where there is little possibility that the eruption itself modified the tropical ENSO state (e.g., Maher et al. 2015). The height of the bars shows the vertically averaged SAM index over the year following the eruption (from June 1991 to May 1992), and we note that the conclusions are not dependent on the exact averaging period or the levels over which the vertical average is taken. Models that were experiencing La Niña conditions at the time of the eruption (blue shading) all show large SAM indices over the following year. The five models that were experiencing El Niño conditions (red shading) exhibit significantly weaker SAMs, but four of the five still show positive SAM indices. One would expect these models to exhibit negative SAMs if El Niño was acting alone. Thus, while none of the 14 models analyzed here exhibited a negative SAM as strong as the one in the reanalysis, the correlation between the SAM index and the Niño-3.4 index across the models is −0.61, at least suggestive that the state of ENSO may have played a role in masking the positive SAM response to Pinatubo.

We conclude by noting that 9 of the 14 models were experiencing La Niña–like conditions (negative Niño-3.4 index) in June–August 1991. Thus, it is possible that

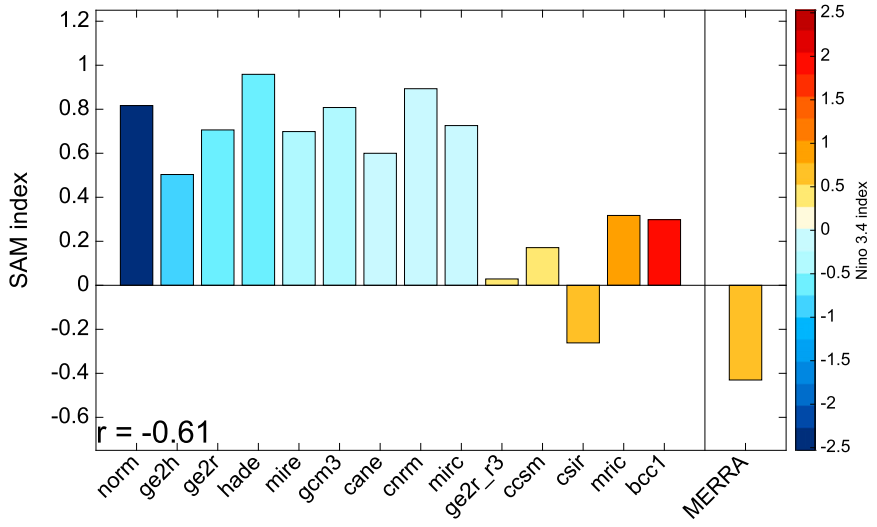

FIG. 10. Vertically averaged SAM index over the year following the Pinatubo eruption (from June 1991 to May 1992) for each of the CMIP5 models and MERRA. Colors denote the Niño-3.4 index averaged between June and August 1991, with models ordered from smallest to largest. The across-model correlation between the mean Niño-3.4 index and mean SAM index is denoted in the bottom left-hand corner.

the tropospheric SAM-like response seen in July immediately following the eruption (e.g., Fig. 5a) may be due to this coincidence. This may also explain why the circulation anomalies weaken in August and reappear in September, when the radiative response to the eruption has had time to develop and when the stratospheric anomalies have coupled to the troposphere.

6. Conclusions

We analyzed the circulation and precipitation responses in 14 different CMIP5 models following the eruption of Mount Pinatubo in June 1991. Although all months exhibited significant and robust circulation and precipitation anomalies in the year following the eruption, the anomalies were not fixed in space nor did they fall into typical seasonal categories (i.e., the strongest responses were found in the following November and December). We identified robust responses across the models using two methods: the statistical significance of the anomalies and the degree to which the models agreed on the sign of the response. The main results from the CMIP5 simulations are summarized as follows:

1) The temperature, circulation, and precipitation all exhibit robust anomalies in both hemispheres in the 8 months following the eruption.
2) The Northern Hemisphere troposphere exhibits robust North Atlantic and North Pacific responses, with the largest response appearing in the cool months approximately 5 months later (November).
3) The Northern Hemisphere circulation response does not project well onto the NAM; however, an alternative diagnostic allowing for a latitudinal shift in the pattern is shown to better capture the response throughout the troposphere.
4) The Southern Hemisphere troposphere exhibits a robust SAM-like response in the year following the eruption, with the largest anomalies appearing in the summer approximately 5 months later (November).
5) The magnitude of the Southern Hemisphere SAM response may be masked by the tropical ENSO conditions during and immediately following the eruption, potentially explaining the discrepancy between the models and observations.

While it is well documented that the Northern Hemisphere tropospheric response to volcanic eruptions is that of a positive NAO/NAM, the response in the Southern Hemisphere has been less clear. Perlwitz and Graf (1995) described the basic mechanism linking volcanic eruptions to Northern Hemisphere tropospheric circulation changes through a strengthening of the polar vortex, and one might expect that dynamically the Southern Hemisphere should respond similarly. In accordance with this, we demonstrated a robust positive SAM response to the Mount Pinatubo eruption across the CMIP5 models. Thus, it is likely that the planetary wave dynamics outlined by Perlwitz and Graf (1995) also apply to the Southern Hemisphere response [see discussion by Karpechko et al. (2010)]. Furthermore, while it is possible that model biases in polar vortex

strength may modify the CMIP5 models' circulation response as suggested by Ottera (2008) and Stenchikov et al. (2006), such effects do not appear to dominate the CMIP5 model responses.

Robock et al. (2007) found no tropospheric SAM response to Mount Pinatubo in an earlier version of the NASA GISS model, and we speculate that this may have been because of internal climate variability (e.g., the state of ENSO) and/or the seasonal focus (JJA only) of that study. Results presented here suggest that the Southern Hemisphere tropospheric response maximizes in November and does not fall into the typical 3-month seasonal averages. Driscoll et al. (2012) argued that the CMIP5 models were unable to simulate the Northern Hemisphere tropospheric response to volcanic eruptions, while here we find a robust circulation response in both the North Atlantic and North Pacific. A possible reason for these differences may be that they composited multiple eruptions, while here we focus solely on the circulation following the Mount Pinatubo eruption. Differences in stratospheric ozone during the different periods of eruptions analyzed by Driscoll et al. (2012) may at least partially account for the differences between our and their results, since Muthers et al. (2014) suggest that the climate response is sensitive to ozone climatology. Furthermore, Driscoll et al. (2012) employed 3-month seasonal averages and averaged the periods after 2 postvolcanic winters. Here, we find no model agreement in the tropospheric response after the first year, and so the 2-yr average may also have muted the responses shown in Driscoll et al. (2012).

The CMIP5 models demonstrate that great care must be taken in diagnosing volcanically forced tropospheric circulation responses. The anomalies may not be well captured by the annular mode indices, and thus, alternative metrics may be required to document the response. Additionally, internal climate variability such as ENSO may partially or wholly mask the forced response to any one eruption in the observations. However, given that the response may depend on the ozone climatology at the time (Muthers et al. 2014), compositing results across multiple eruptions to remove climate noise may in fact complicate matters. Furthermore, Christiansen (2008) analyzed a series of observations of volcanic periods and suggested a possible link between volcanic eruptions and ENSO—namely, that the climate response to the eruptions may force an ENSO response. While Ding et al. (2015) suggest that there is no compelling link between volcanic eruptions and ENSO in the CMIP5 ensemble, another analysis of CMIP5 models by Maher et al. (2015) concludes that volcanic eruptions can affect ENSO. Thus, any analysis of the impacts of climate variability on the circulation response to volcanic eruptions will need to additionally consider the possibility of feedbacks onto the variability itself.

Acknowledgments. We thank Haibo Liu and the Lamont-Doherty Earth Observatory for obtaining the CMIP5 data and the World Climate Research Programme's Working Group on Coupled Modelling, which is responsible for CMIP. We also thank the climate modeling groups for producing and making available their model output. For CMIP the U.S. Department of Energy's Program for Climate Model Diagnosis and Intercomparison provides coordinating support and led development of software infrastructure in partnership with the Global Organization for Earth System Science Portals. MERRA data used in this study have been provided publicly by the Global Modeling and Assimilation Office (GMAO) at NASA Goddard Space Flight Center through the NASA GES DISC online archive. This work was supported, in part, by the Climate and Large-Scale Dynamics Program of the National Science Foundation (NSF) under Grant 1419818. LMP is also funded, in part, by a grant from the NSF. SS acknowledges support under NSF Grant 1419667.

REFERENCES

Baldwin, M. P., and T. J. Dunkerton, 1999: Propagation of the Arctic Oscillation from the stratosphere to the troposphere. *J. Geophys. Res.*, **104**, 30 937–30 946, doi:10.1029/1999JD900445.

Barnes, E. A., N. W. Barnes, and L. M. Polvani, 2014: Delayed Southern Hemisphere climate change induced by stratospheric ozone recovery, as projected by the CMIP5 models. *J. Climate*, **27**, 852–867, doi:10.1175/JCLI-D-13-00246.1.

Christiansen, B., 2008: Volcanic eruptions, large-scale modes in the Northern Hemisphere, and the El Niño–Southern Oscillation. *J. Climate*, **21**, 910–922, doi:10.1175/2007JCLI1657.1.

Deshler, T., 2008: A review of global stratospheric aerosol: Measurements, importance, life cycle, and local stratospheric aerosol. *Atmos. Res.*, **90**, 223–232, doi:10.1016/j.atmosres.2008.03.016.

Ding, Y., J. A. Carton, G. A. Chepurin, G. Stenchikov, A. Robock, L. T. Sentman, and J. P. Krasting, 2015: Ocean response to volcanic eruptions in Coupled Model Intercomparison Project 5 simulations. *J. Geophys. Res. Oceans*, **119**, 5622–5637, doi:10.1002/2013JC009780.

Driscoll, S., A. Bozzo, L. Gray, A. Robock, and G. Stenchikov, 2012: Coupled Model Intercomparison Project 5 (CMIP5) simulations of climate following volcanic eruptions. *J. Geophys. Res.*, **117**, D17105, doi:10.1029/2012JD017607.

Efron, B., 1979: Bootstrap methods: Another look at the jackknife. *Ann. Stat.*, **7**, 1–26, doi:10.1214/aos/1176344552.

Graf, H., I. Kirchner, A. Robock, and I. Schult, 1993: Pinatubo eruption winter climate effects: Model versus observation. *Climate Dyn.*, **9**, 81–93, doi:10.1007/BF00210011.

Karpechko, A., N. P. Gillett, M. Dall'Amico, and L. J. Gray, 2010: Southern Hemisphere atmospheric circulation response to the El Chichón and Pinatubo eruptions in coupled climate models. *Quart. J. Roy. Meteor. Soc.*, **136**, 1813–1822, doi:10.1002/qj.683.

Kodera, K., H. Chiba, A. Koide, A. Kitoh, and Y. Nikaidou, 1996: Interannual variability of the winter stratosphere and troposphere in the Northern Hemisphere. *J. Meteor. Soc. Japan*, **74**, 365–382.

Lehner, F., A. P. Schurer, G. C. Hegerl, C. Deser, and L. Thomas, 2016: The importance of ENSO phase during volcanic eruptions for detection and attribution. *Geophys. Res. Lett.*, **43**, 2851–2858, doi:10.1002/2016GL067935.

L'Heureux, M., and D. Thompson, 2006: Observed relationships between the El Niño–Southern Oscillation and the extratropical zonal-mean circulation. *J. Climate*, **19**, 276–287, doi:10.1175/JCLI3617.1.

Maher, N., S. McGregor, M. H. England, and A. S. Gupta, 2015: Effects of volcanism on tropical variability. *Geophys. Res. Lett.*, **42**, 6024–6033, doi:10.1002/2015GL064751.

Muthers, S., and Coauthors, 2014: Northern Hemispheric winter warming pattern after tropical volcanic eruptions: Sensitivity to the ozone climatology. *J. Geophys. Res. Atmos.*, **119**, 1340–1355, doi:10.1002/2013JD020138.

Ortega, P., F. Lehner, D. Swingdouw, V. Masson-Delmotte, C. C. Raible, M. Casado, and P. Yiou, 2015: A model-tested North Atlantic Oscillation reconstruction for the past millennium. *Nature*, **523**, 71–74, doi:10.1038/nature14518.

Ottera, O. H., 2008: Simulating the effects of the 1991 Mount Pinatubo volcanic eruption using the ARPEGE atmosphere general circulation model. *Adv. Atmos. Sci.*, **25**, 213–226, doi:10.1007/s00376-008-0213-3.

Perlwitz, J., and H.-F. Graf, 1995: The statistical connection between tropospheric and stratospheric circulation of the Northern Hemisphere in winter. *J. Climate*, **8**, 2281–2295, doi:10.1175/1520-0442(1995)008<2281:TSCBTA>2.0.CO;2.

Rienecker, M. M., and Coauthors, 2011: MERRA: NASA's Modern-Era Retrospective Analysis for Research and Applications. *J. Climate*, **24**, 3624–3648, doi:10.1175/JCLI-D-11-00015.1.

Robock, A., 2000: Volcanic eruptions and climate. *Rev. Geophys.*, **38**, 191–219, doi:10.1029/1998RG000054.

——, and J. Mao, 1995: The volcanic signal in surface temperature observations. *J. Climate*, **8**, 1086–1103, doi:10.1175/1520-0442(1995)008<1086:TVSIST>2.0.CO;2.

——, T. Adams, M. Moore, L. Oman, and G. Stenchikov, 2007: Southern Hemisphere atmospheric circulation effects of the 1991 Mount Pinatubo eruption. *Geophys. Res. Lett.*, **34**, L23710, doi:10.1029/2007GL031403.

Roscoe, H., and J. Haigh, 2007: Influences of ozone depletion, the solar cycle and the QBO on the southern annular mode. *Quart. J. Roy. Meteor. Soc.*, **133**, 1855–1864, doi:10.1002/qj.153.

Rozanov, E. V., M. E. Schlesinger, N. G. Andronova, F. Yang, S. L. Malyshev, V. A. Zubov, T. A. Egorova, and B. Li, 2002: Climate/chemistry effects of the Pinatubo volcanic eruption simulated by the UIUC stratosphere/troposphere GCM with interactive photochemistry. *J. Geophys. Res.*, **107**, 4594, doi:10.1029/2001JD000974.

Santer, B. D., and Coauthors, 2013a: Identifying human influences on atmospheric temperature. *Proc. Natl. Acad. Sci. USA*, **110**, 26–33, doi:10.1073/pnas.1210514109.

——, and Coauthors, 2013b: Human and natural influences on the changing thermal structure of the atmosphere. *Proc. Natl. Acad. Sci. USA*, **110**, 17 235–17 240, doi:10.1073/pnas.1305332110.

Solomon, S., 1999: Stratospheric ozone depletion: A review of concepts and history. *Rev. Geophys.*, **37**, 275–316, doi:10.1029/1999RG900008.

Stenchikov, G., K. Hamilton, A. Robock, V. Ramaswamy, and M. D. Schwarzkopf, 2002: Arctic Oscillation response to the 1991 Pinatubo eruption: Effects of volcanic aerosols and ozone depletion. *J. Geophys. Res.*, **107**, 4803, doi:10.1029/2002JD002090.

——, ——, R. J. Stouffer, A. Robock, V. Ramaswamy, B. Santer, and H.-F. Graf, 2006: Arctic Oscillation response to volcanic eruptions in the IPCC AR4 climate models. *J. Geophys. Res.*, **111**, D07107, doi:10.1029/2005JD006286.

Taylor, K. E., R. J. Stouffer, and G. A. Meehl, 2012: An overview of CMIP5 and the experiment design. *Bull. Amer. Meteor. Soc.*, **93**, 485–498, doi:10.1175/BAMS-D-11-00094.1.

Thomas, M., C. Timmreck, M. Giorgetta, H.-F. Graf, and G. Stenchikov, 2009: Simulation of the climate impact of Mt. Pinatubo eruption using ECHAM5—Part 1: Sensitivity to the modes of atmospheric circulation and boundary conditions. *Atmos. Chem. Phys.*, **9**, 757–769, doi:10.5194/acp-9-757-2009.

Thompson, D. W. J., S. Solomon, P. J. Kushner, M. H. England, K. M. Grise, and D. J. Karoly, 2011: Signatures of the Antarctic ozone hole in Southern Hemisphere surface climate change. *Nat. Geosci.*, **4**, 741–749, doi:10.1038/ngeo1296.

Timmreck, C., 2012: Modeling the climatic effects of large explosive volcanic eruptions. *Wiley Interdiscip. Rev.: Climate Change*, **3**, 545–564, doi:10.1002/wcc.192.